Critical single-domain/multidomain grain sizes in noninteracting and interacting elongated magnetite particles: Implications for magnetosomes

Critical single-domain/multidomain grain sizes in noninteracting and interacting elongated magnetite particles: Implications for magnetosomes

Adrian R. Muxworthy[1,2] and Wyn Williams[3]

Received 21 June 2006; revised 3 October 2006; accepted 20 October 2006; published 30 November 2006.

[1] The critical size for stable single-domain (SD) behavior has been calculated as a function of grain elongation for magnetite grains using a numerical micromagnetic algorithm. Importantly, for the first time, we consider the contribution of intergrain magnetostatic interactions on the SD/multidomain (MD) critical size (d_0). For individual grains our numerical estimates for d_0 for elongated grains are lower than that determined by previous analytical and numerical calculations. Nevertheless, the inclusion of magnetostatic interactions into the model was found to increase d_0 to values significantly higher than any previously published estimates of d_0 for individual grains. Therefore the model calculations show that there is a relatively wide range of grain sizes within which depending on the degree of magnetostatic interactions and elongation, a grain can be either SD or MD. The model results are compared to observations of magnetosomes found in magnetotactic bacteria. The newly calculated upper d_0 limit for the interacting grains now accommodates the largest magnetosomes reported in the literature. These large magnetosomes were previously thought to be MD, suggesting that evolutionary processes are highly efficient at optimizing magnetosome grain size and spatial distribution.

Citation: Muxworthy, A. R., and W. Williams (2006), Critical single-domain/multidomain grain sizes in noninteracting and interacting elongated magnetite particles: Implications for magnetosomes, *J. Geophys. Res.*, *111*, B12S12, doi:10.1029/2006JB004588.

1. Introduction

[2] The transition from single-domain (SD) to multidomain (MD) magnetic behavior is highly important to magnetists as it marks the switch from relatively stable to unstable magnetization and is an important indicator of grain size. For earth scientists the SD/MD critical size (d_0) for magnetite is of particular interest due to magnetite's abundance and large spontaneous magnetization (M_S). In a much cited paper, *Butler and Banerjee* [1975] calculated d_0 as a function of the grain elongation axial ratio AR (short axis/long axis or length/width) for parallelepiped magnetite using an analytical approach based on *Amar*'s [1958] modifications of *Kittel*'s [1949] theories.

[3] Since these papers were published there have been rapid advances in computing resources, allowing for *Brown*'s [1963] micromagnetic equations to be solved numerically. Micromagnetic studies have shown that the analytical approach adopted by *Butler and Banerjee* [1975], which assumes uniform SD structures and simple two-domain structures is over simplified for soft magnetic materials like magnetite [e.g., *Williams and Dunlop*, 1989; *Fabian et al.*, 1996]. Instead, large SD grains are magnetically nonuniform and display "flowering" toward the edge of the grains (Figure 1a), while the smallest MD grains do not display two distinct domains with a separating domain wall, but curling vortex structures (Figure 1b).

[4] Using micromagnetic simulations, several previous studies have calculated d_0 versus AR for single crystals with various anisotropies [*Fabian et al.*, 1996; *Newell and Merrill*, 1999; *Witt et al.*, 2005]. In addition, *Rave et al.* [1998] determined d_0 versus variable uniaxial anisotropy; variable uniaxial anisotropy can be thought of as being similar to variable elongation. The most recent study by *Witt et al.* [2005] made d_0 versus AR micromagnetic calculations for individual parallelepiped and magnetosome-shaped magnetite particles. Their interest in magnetosomes is driven by the generally assumed idea that it is beneficial for magnetosomes to evolve to maximum SD sizes. They found that the magnetosome shape increased d_0 compared to the parallelepipeds, to accommodate all the grain size and grain shape observations of *Petersen et al.* [1989]. In contrast, the parallelepiped calculations did not. Nevertheless, the model of *Witt et al.* [2005] does not explain the existence from a magnetic view point of the largest magnetosomes reported in the literature, for example, the large coccoid Itaipu-1 magnetosomes that are up to 250 nm in

[1] GeoForschungsZentrum Potsdam, Potsdam, Germany.
[2] Permanently at Department of Earth Science and Engineering, Imperial College, London, UK.
[3] Grant Institute of Earth Science, University of Edinburgh, Edinburgh, UK.

0148-0227/06/2006JB004588$09.00

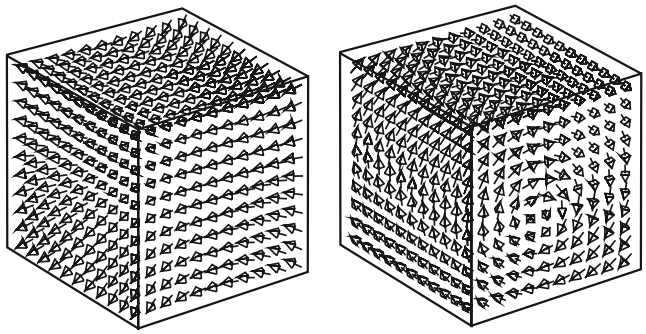

Figure 1. Domains states occurring in cubic grains of magnetite at room temperature for a grain with edge length of 100 nm (a) single-domain (flower state) and (b) single-vortex state. In this paper the term ''SD state'' refers not just to homogeneous magnetization structures but also to nonuniform domain structures as shown in Figure 1a which are essentially SD-like with a degree of flowering toward the edges of the grain. In Figures 1a and 1b the crystallographic $\langle 100 \rangle$ is aligned with the x axis.

length, with a maximum width of 210 nm (AR = 0.84) [*Spring et al.*, 1998; *McCartney et al.*, 2001; *Lins et al.*, 2005].

[5] However, these direct comparisons between d_0 calculations for individual magnetosomes and most experimental observations are flawed, because magnetosomes nearly always occur in magnetostatically interacting chains. Magnetostatic interactions are known to strongly affect magnetic behavior [*Shcherbakov and Shcherbakova*, 1975; *Muxworthy et al.*, 2003].

[6] In this paper we use a micromagnetic algorithm to calculate d_0 for individual and magnetostatically interacting chains of elongated magnetite crystals. In addition to magnetostatic interactions we consider the importance of the relative orientation of magnetite's cubic magnetocrystalline anisotropy with respect to grain elongation.

2. Micromagnetic Algorithm

[7] The model subdivides a grain into a number of subcubes. Each subcube represents the averaged magnetization direction of many hundreds of atomic magnetic dipole moments. All the subcubes have equal magnetic magnitude, but their magnetization can vary in direction (Figure 1).

[8] To determine the magnetic structures using this finite difference model, two approaches were considered; a combination of both a conjugate gradient (CG) algorithm [*Williams and Dunlop*, 1989] and a dynamic algorithm [*Suess et al.*, 2002; *Williams et al.*, 2006], and the CG algorithm alone. The reasoning behind the combination approach is that the dynamic algorithm gives the more rigorous solution, however, it is relatively slow compared to the CG method. In the combination algorithm, we use the CG algorithm to generate rapidly a magnetic structure, which is then put into the dynamic solver as an initial guess. This increases the efficiency of the algorithm by roughly an order of magnitude compared to the dynamic solver alone. The use of the CG algorithm by itself is discussed below.

[9] In the CG algorithm the domain structure is calculated by minimizing the total magnetic energy E_{tot}, which is the sum of the exchange energy E_{ex} proportional to the exchange constant A, magnetostatic energy E_d proportional to the spontaneous magnetization M_S, and the anisotropy E_{anis} proportional to the first magnetocrystalline anisotropy K_1 [*Brown*, 1963]. E_{tot} is calculated using fast Fourier transforms (FFT), to give a local energy minimum (LEM) for the assemblage. The FFT is required to calculate the demagnetizing energy, which allows the high resolution needed to examine large arrays of interacting grains. Values for A, M_S and K_1 were taken from *Heider and Williams* [1988], *Pauthenet and Bochirol* [1951], and *Fletcher and O'Reilly* [1974], respectively.

[10] In the combination algorithm after the LEM state has been estimated, the structure is minimized by the dynamic algorithm [*Suess et al.*, 2002]. This algorithm solves the dynamic Landau-Lifshitz-Gilbert equation. We used a finitely damped solver detailed by *Brown et al.* [1989]. In effect, instead of minimizing the energy, the solver minimizes the torque on each magnetic moment by solving for the effective field.

[11] The initial CG ''guess'' for magnetic structures of the most elongated grains was found to be effectively the same as the solution produced by the dynamic solver. This convergence between the two algorithms is due to smoothing of the energy surfaces as the grains become more elongated. For more symmetrical grains with more uneven energy surfaces, the CG algorithm can become hooked on small saddle points and trapped in shallow minimum energy states. Therefore, as the grains become more elongated, the CG algorithm is less likely to stall and the CG and dynamic solutions converge. Because the CG solver is approximately an order of magnitude faster than the combined algorithm, and more memory efficient than the dynamic algorithm, for some of the larger arrays, i.e., for the largest chains of elongated grains, calculations were made using only the CG algorithm.

[12] To accurately model nonuniform structures, it is necessary to have a minimum model resolution of two cells per exchange length (exchange length equal to $\sqrt{(A/K_d)}$, where $K_d = \mu_0 M_s^2/2$ and μ_0 is the permeability of free space [*Rave et al.*, 1998]). The minimum resolution was implemented at all times in this paper.

[13] The modeling of interactions in this paper was simply done by masking out blank cells, setting the cells' magnetization to zero, and thereby creating a 'void' between neighboring magnetic regions of our finite difference mesh [*Muxworthy et al.*, 2003].

3. SD/MD Critical Sizes for Individual Elongated Grains

[14] There are several methods of determining the SD/MD critical size. Here the unconstrained method is employed [*Fabian et al.*, 1996; *Wright et al.*, 1997; *Witt et al.*, 2005]. In this approach a very small grain, say ~20 nm in length, with an initial SD structure is gradually increased in size until the domain structure collapses to a vortex structure, i.e., MD, at d_{max} (Figure 2). The grain size is

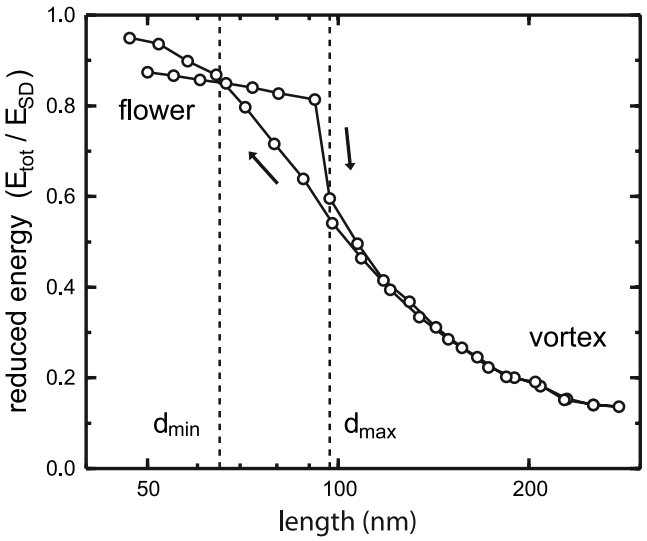

Figure 2. Magnetic energy density of a magnetite cube as a function of length for an initial SD configuration at room temperature (Figure 1a). The grain size was gradually increased until the SD structure collapsed into a vortex structure (Figure 1b) at d_{max} = 96 nm. The size was then gradually decreased until a SD state formed at d_{min} = 64 nm. To maximize computer efficiency, the resolution was increased/decreased with each increase/decrease in size, and the domain structure was rescaled between each pair of calculations.

then decreased until the vortex structure becomes SD at d_{min} (Figure 2). The d_{min} and d_{max} are interpreted as the lower and upper bounds of a range where both SD and vortex structures can coexist. For the most elongated grains, i.e., AR < 0.4, d_{min} and d_{max} were poorly defined, as the collapse is gradual and less abrupt. In such cases d_{min} and d_{max} were taken to be when the normalized magnetization passed through 0.8 on the increasing/decreasing curves (Figure 2), where the normalized magnetization is the magnetic moment divided by magnetic moment of an ideal SD grain.

[15] In addition to calculating d_{min} and d_{max} as a function of AR (Figure 3), we have considered the relationship between the relative orientation of magnetite's cubic magnetocrystalline anisotropy and the elongation. We model the two extreme cases; first, where the elongation is in the ⟨100⟩ direction (d^{100}_{min} and d^{100}_{max}) and second in the ⟨111⟩ direction (d^{111}_{min} and d^{111}_{max}). The easy axes for magnetite's magnetocrystalline anisotropy at room temperature are the ⟨111⟩ directions. In the ⟨111⟩ scenario the magnetocrystalline anisotropy enhances the shape effect, i.e., it encourages the magnetization to align along the elongation axis, in contrast in the ⟨100⟩ it competes with the shape effect.

[16] In Figure 3, the y axis is the length as used by *Butler and Banerjee* [1975], rather than the mean diameter as used by *Witt et al.* [2005]. The use of the length makes for easier comparison with Butler and Banerjee, but Figure 3 is a little more complicated to understand, because on moving horizontally across Figure 3 the volume of the grains changes; that is, there is a change both in shape contributing to d_0 and in volume contributing to d_0.

[17] Generally, d^{100}_{min}, d^{100}_{max}, d^{111}_{min} and d^{111}_{max} all increase as AR decreases (Figure 3). The d^{111}_{max} is larger than d^{100}_{min}, d^{100}_{max} and d^{111}_{min} for all values of AR. Orienting the magnetocrystalline anisotropy along ⟨111⟩ enhances the effect of elongation, while orienting in the ⟨100⟩ orientation increases curling of the magnetization at the edges of the grains, i.e., breaking the symmetry, which encourages nucleation of vortex states decreasing d_0. As AR is reduced the difference between d^{100}_{min} and d^{100}_{max} decreases, similarly with d^{111}_{min} and d^{111}_{max} as d_{min} and d_{max} become less well defined and the curve as shown in Figure 2 becomes reversible.

[18] For comparison the theoretical model of *Butler and Banerjee* [1975] is depicted (Figure 3). It is seen that the

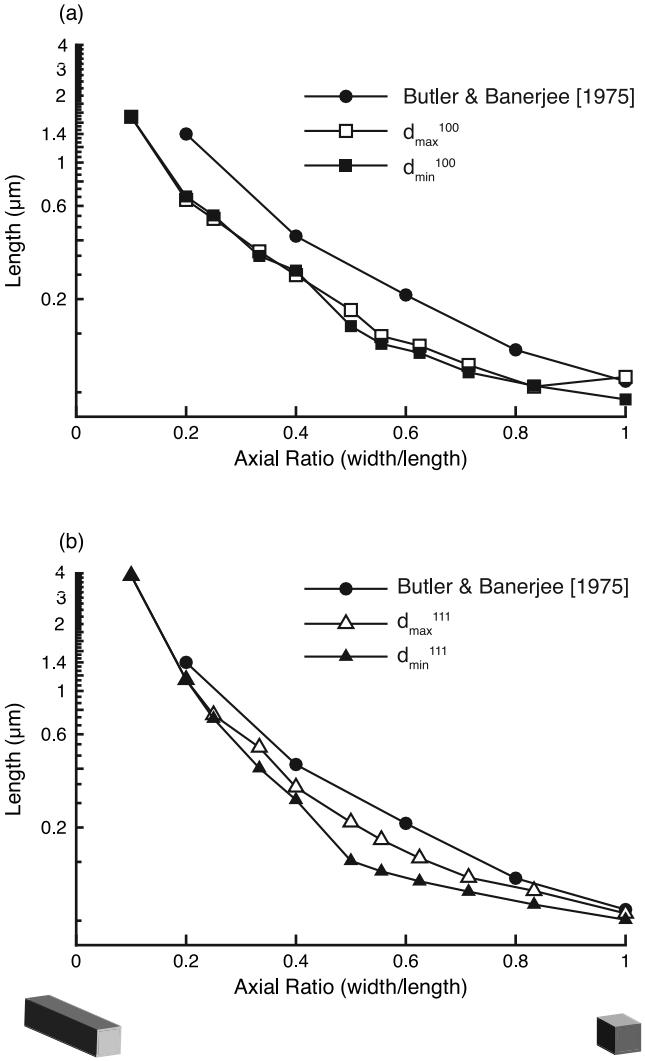

Figure 3. Critical SD to MD lengths (maximum grain dimension) for individual grains of magnetite as a function of axial ratio AR. Elongation along (a) the ⟨100⟩ direction and (b) the ⟨111⟩ direction. Both d_{max} and d_{min} are shown. These were determined using the method as defined in Figure 2. For the very elongated grains, i.e., AR < 0.5, d_{max} and d_{min} were poorly defined. For these smaller values of AR, d_{max} and d_{min} were defined as the length where the reduced magnetization passed through 0.8 on increasing/decreasing grain size. AR = 1 is a cube, and AR = 0 is an infinitely long parallelepiped.

micromagnetic estimates are significantly below the analytical model.

[19] *Witt et al.* [2005] calculated d^{100}_{min} and d^{100}_{max} for parallelepiped and d^{111}_{min} and d^{111}_{max} for magnetosome shapes using the same unconstrained approach. For the parallelepipeds their values were very similar to those of *Fabian et al.* [1996]. Compared to this study, their estimates for d^{100}_{min} are approximately the same, but much higher for d^{100}_{max}. Although not directly comparable due to the difference in shape between parallelepipeds and magnetosomes, *Witt et al.* [2005] estimated lower and higher values for d^{111}_{min} and d^{111}_{max}, respectively. We believe that these differences between the two studies are due to two significant variations in the algorithms. First, *Witt et al.* [2005] and other similar studies [e.g., *Fabian et al.*, 1996] used only the CG algorithm. In this study the more robust combined algorithm was used for all the calculations shown in Figure 3 for AR > 0.1. As discussed above the CG algorithm is prone to becoming trapped in false energy states (particularly for high values of AR), which using the unconstrained method for determining critical sizes would lead to an overestimate of d_{max} and an underestimate of d_{min}. Second, *Witt et al.* [2005] used a constant resolution during their simulations, which is likely to underestimate the exchange energy for the larger grains, leading to an underestimation of both d_{min} and d_{max}. In this study the minimum exchange length was used at all times, rescaling the solutions between different calculations.

4. SD/MD Critical Sizes for Magnetostatically Interacting Elongated Grains

[20] To model the effect of magnetostatic interactions on d_0, we consider the behavior of the middle grain in a chain of three grains (Figure 4). We examine the behavior of chains as opposed to a three-dimensional grid, as this is likely to produce the largest difference compared to noninteracting grains [*Muxworthy and Williams*, 2004] and allows for direct comparison with magnetotatic bacteria observations. A chain of three grains is short, however, it was chosen so that we could calculate d_0 for elongated grains with large intergrain spacings using a full resolution model. For example, the largest solutions considered had ~1.8 million elements. The minimum AR was 0.33.

[21] To estimate d_0, a slightly different procedure to section 3 was utilized. Rather than growing the domain structure, at each grain size an initial SD state was assumed, and the model structure minimized. This procedure produces only a single value for d_0. As in section 4, the orientation of the magnetocrystalline anisotropy is considered, i.e., d^{100} and d^{111}. All three grains in the chain had the same magnetocrystalline anisotropy orientation.

[22] Determining d_0 as both a function of AR and grain spacing produces a three-dimensional surface plot (Figure 4). We consider a minimum nontouching separation of spacing/length equal to 0.05 and calculate d_0 for touching grains, i.e., space/length equal to 0.0. The noninteracting data (section 3) is plotted at spacing/length distance of 3. It is readily seen that both elongation and magnetostatic interactions significantly increase both d^{100} and d^{111} (Figure 4). On comparison between Figures 4a and 4b it is seen that d^{100} is slightly lower than d^{111}.

5. Implications for Magnetotatic Bacterial Studies

[23] In recent years there has been a great interest in magnetotatic bacteria, both in the bacteria themselves [e.g., *Petersen et al.*, 1989; *Arató et al.*, 2005] and of the possibility of using the identification of fossil magnetosomes in meteorites thought to come from Mars as indicators for extraterrestrial life [e.g., *Taylor et al.*, 2001; *Weiss et al.*, 2004]. Several studies have compared observational data for magnetosomes or the magnetite crystals found in meteorites with the d_0 model of *Butler and Banerjee* [1975]. The reasoning behind this comparison is that while the production of magnetite may have potentially several uses, one of which is navigation, it is clear that through optimization magnetosomes must still retain their ability to act as a compasses, i.e., be SD. In particular, it is thought to be advantageous for magnetosomes to evolve to be just a little smaller than d_0. As shown above in sections 3 and 4, the analytical calculations of *Butler and Banerjee* [1975] overestimate d_0 for isolated elongated crystals but did not include magnetostatic interactions. As magnetosomes commonly occur as closely spaced magnetostatically interacting chains, the application of the *Butler and Banerjee* [1975] model is inappropriate.

[24] In Figure 5, we assess the magnetic stability of published observational data by comparing it to the calculations from sections 3 and 4. The model data in the previous sections is reduced to the minimum d_{min}, i.e., d^{100}_{min} and the maximum d_{max} i.e., d^{111}_{max} for the noninteracting grains, and the maximum d_0 for the interacting grains, i.e., d^{111}_{max}, both for the nontouching (spacing/length equal to 0.05) and touching (spacing/length equal to 0.00).

[25] We consider three sets of magnetosome observation data. First, the data of *Arató et al.* [2005], from which we have selected (1) interacting magnetosomes from Séd stream in Hungary residing in double chains and (2) Malom-tó (mill pond) magnetosomes which are scattered. The interaction fields between the double Séd chains are likely to be very small compared to the interaction field within the chains, effectively making the two chains magnetically independent. The Séd magnetosomes cluster in the interacting region (Figure 3). In contrast the Malom-tó magnetosomes plot below in the ''noninteracting'' zone. The largest Malom-tó grains follow d_{max} closely, with no Malom-tó magnetosomes (sample size 241) plotting above d_{max}. While the Malom-tó grains may still experience some

Figure 4. The d_0 surfaces for interacting chains of elongated magnetite; grain spacing/length versus AR versus length elongation along (a) the ⟨100⟩ direction and (b) the ⟨111⟩ direction. The d_0 was determined from the behavior of the middle grain in a chain of three identical grains with various intergrain spacings. The spacing is divided by the grain length. The data for the individual grains has been placed at a spacing/length equal to 3. The first calculated point for chains is set at a spacing/length equal to 2. Because of insufficient computing memory, no calculation of d_0 was made for the point with spacing/length equal to 0.0 and AR = 0.33.

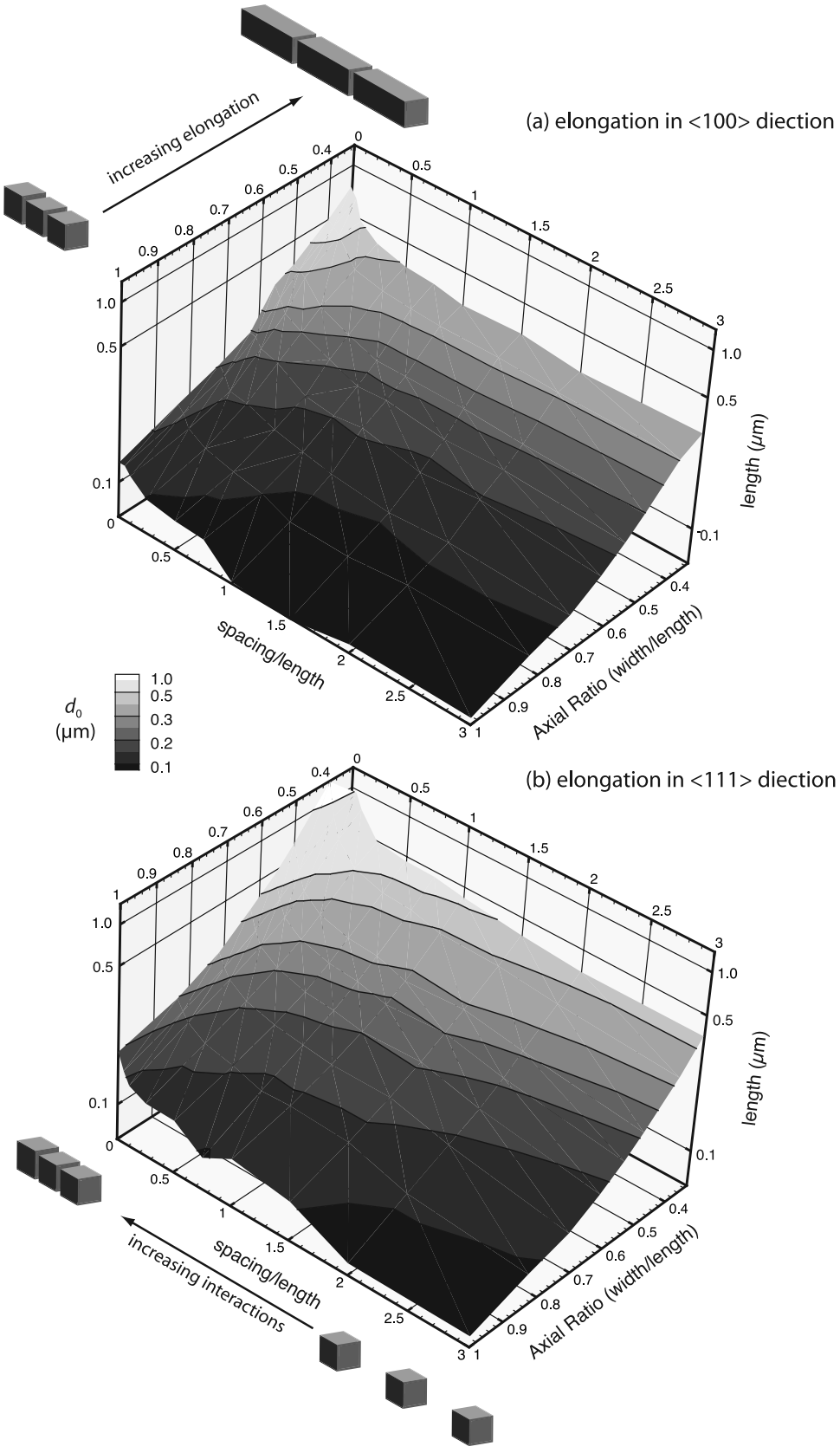
(a) elongation in <100> diection
increasing elongation
spacing/length
Axial Ratio (width/length)
length (μm)
d_0 (μm)
1.0
0.5
0.3
0.2
0.1
(b) elongation in <111> diection
increasing interactions
spacing/length
Axial Ratio (width/length)
length (μm)

Figure 4

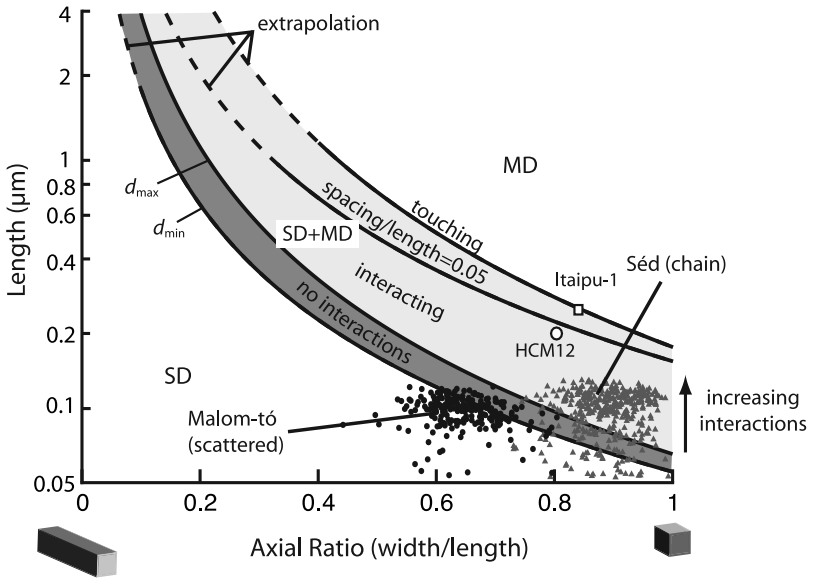

Figure 5. The d_0 for length versus AR for the minimum noninteracting d_{min}, the maximum noninteracting d_{max}, and the maximum d_0 for the interacting systems shown in Figure 4 (spacing/length equal to 0 (touching) and 0.05). The models are shown previously in Figures 3 and 4. Power law fits have been made to the data. Power law fits (solid lines) and extrapolations (dashed lines) have been made to the data. Observational data for various magnetosome data are plotted; Séd and Malom-tó data are from *Arató et al.* [2005], HCM12 [from *Taylor and Barry*, 2004] and Itaipu-1 [*Spring et al.*, 1998; *McCartney et al.*, 2001; *Lins et al.*, 2005] are the largest magnetosomes that we have found in the literature. The highlighted ''interacting'' region is an upper bound. It is possible for magnetosomes to be smaller, interacting and stable SD, i.e., to plot below this region. The ''interacting'' region is the region where the grains must be interacting to be stable SD. The exact upper limit is dependent on spacing and elongation. AR = 1 is a cube, and AR = 0 is an infinitely long parallelepiped.

intermagnetosome magnetostatic interaction fields, they will not be subjected to the strong linear or ''positive'' interactions experienced by the Séd magnetosomes. So, although not truly ''noninteracting'' because of the random nature of the interaction field, it is highly unlikely that in some way the bacteria has evolved to maximize the grain size with the use of this dispersed interaction field.

[26] It might initially appear that the Séd magnetosomes are evolutionary more developed than the Malom-tó magnetosomes from the point of view of magnetosome size. However, as magnetotactic bacteria are thought to have evolved in the early Proterozoic [*Chang and Kirschvink*, 1989], the reasons why magnetotactic bacteria like Malom-tó do not display magnetosomes in chains, must be due to minimal evolutionary advantage in some environments.

[27] Two further data sets were considered. These were the largest magnetosomes that we were able to identify in the literature [*Spring et al.*, 1998; *McCartney et al.*, 2001; *Taylor and Barry*, 2004; *Lins et al.*, 2005], and they are both marine in origin and are depicted in Figure 5. The coccobacillus HCM12 sample [*Taylor and Barry*, 2004] contains ''pseudohexagonal'' prismatic magnetosomes of length of 200 nm and AR = 0.8. The magnetosomes have a spacing/length ~0.05. This sample plots just below the upper d_0 limit for chains with an interaction spacing/length of 0.05 (Figure 5). The coccoid Itaipu-1 magnetosomes are up to 250 nm in length, with a maximum width of 210 nm (AR = 0.84) and a spacing/length ~0.01 [*Spring et al.*, 1998; *McCartney et al.*, 2001; *Lins et al.*, 2005]. These magnetosomes plot on the very upper limit of d_0 between the curve for spacing/length ~0.05 and the touching model (Figure 5), suggesting the Itaipu-1 magnetosomes have the maximum possible stable SD grain size for their AR.

[28] The calculations demonstrated that even the largest magnetosomes such as HCM12 and Itaipu-1 are likely to exhibit SD rather than MD behavior in the presence of interactions. In the absence of such magnetostatic interactions, these large magnetosomes would be MD. This conclusion is supported by electron holography images of Itaipu-1 magnetosomes [*McCartney et al.*, 2001], which found that when the chains are intact the magnetosomes display SD magnetic structures, but vortex states when broken. This suggests that through evolution, magnetosome size in strains like HCM12 and Itaipu-1 is maximized with the utilization of magnetostatic interactions.

6. Conclusions

[29] There are two main findings in this paper. First, the micromagnetic estimate for d_0 for individual elongated grains is considerably reduced compared to the analytical calculations made by *Butler and Banerjee* [1975] and the upper numerical estimates for d_0, i.e., d_{max}, made by *Witt et al.* [2005]. Second, and more importantly, the role of interactions has been introduced into the model, and it is demonstrated they significantly increase d_0.

[30] For magnetotatic bacteria studies, as the model outlined in the paper accommodates the influence of magne-

tostatic interactions it provides a better estimate for d_0 than the model of *Butler and Banerjee* [1975]. In addition to considering parallelepipeds, *Witt et al.* [2005] made calculations for magnetosome-shaped models, however, on comparison with the results in this study it would appear that the role of interactions is more significant than small variations in shape. The new calculations for d_0, which include magnetostatic interactions, can now accommodate all the published magnetosome data, i.e., even the largest reported magnetosomes will display SD behavior in the presence of interactions.

[31] **Acknowledgments.** This work was funded through NERC grant NE/C510159/1 to W.W. and A.R.M. and Royal Society funding to A.R.M. We would like to thank Mihály Pósfai for providing the raw data from *Arató et al.* [2005].

References

Amar, H. (1958), Size dependence of the wall characteristics in a two-domain iron particle, *J. Appl. Phys.*, *29*, 542–543.

Arató, B., Z. Szányi, C. Flies, D. Schuler, R. B. Frankel, P. R. Buseck, and M. Pósfai (2005), Crystal-size and shape distributions of magnetite from uncultured magnetotactic bacteria as a potential biomarker, *Am. Mineral.*, *90*, 1233–1240.

Brown, P. N., G. D. Byrne, and A. C. Hindmarsh (1989), VODE: A variable coefficient ODE solver, *SIAM J. Sci. Stat. Comput.*, *10*, 1038–1051.

Brown, W. F., Jr. (1963), *Micromagnetics*, John Wiley, Hoboken, N. J.

Butler, R. F., and S. K. Banerjee (1975), Theoretical single-domain grain size range in magnetite and titanomagnetite, *J. Geophys. Res.*, *80*, 4049–4058.

Chang, S.-B. R., and J. L. Kirschvink (1989), Magnetofossils, the magnetization of sediments, and the evolution of magnetite biomineralization, *Annu. Rev. Earth Planet. Sci.*, *17*, 169–195.

Fabian, K., A. Kirchner, W. Williams, F. Heider, T. Leibl, and A. Huber (1996), Three-dimensional micromagnetic calculations for magnetite using FFT, *Geophys. J. Int.*, *124*, 89–104.

Fletcher, E. J., and W. O'Reilly (1974), Contribution of Fe^{2+} ions to the magnetocrystalline anisotropy constant K_1 of $Fe_{3-x}Ti_xO_4(0 < x < 0.1)$, *J. Phys. C*, *7*, 171–178.

Heider, F., and W. Williams (1988), Note on temperature dependence of exchange constant in magnetite, *Geophys. Res. Lett.*, *15*, 184–187.

Kittel, C. (1949), Physical theory of ferromagentic domains, *Rev. Mod. Phys.*, *21*, 541–583.

Lins, U., M. R. McCartney, M. Farina, R. B. Frankel, and P. R. Buseck (2005), Habits of magnetosome crystals in coccoid magnetotactic bacteria, *Appl. Environ. Microbiol.*, *71*, 4902–4905.

McCartney, M. R., U. Lins, M. Farina, P. R. Buseck, and R. B. Frankel (2001), Magnetic microstructure of bacterial magnetite by electron holography, *Eur. J. Mineral.*, *13*, 685–689.

Muxworthy, A. R., and W. Williams (2004), Distribution anisotropy: The influence of magnetic interactions on the anisotropy of magnetic remanence, in *Magnetic Fabric: Methods and Applications*, edited by F. Martín-Hernández et al., *Geol. Soc. Spec. Publ.*, *238*, 37–47.

Muxworthy, A., W. Williams, and D. Virdee (2003), Effect of magnetostatic interactions on the hysteresis parameters of single-domain and pseudosingle-domain grains, *J. Geophys. Res.*, *108*(B11), 2517, doi:10.1029/2003JB002588.

Newell, A. J., and R. T. Merrill (1999), Single-domain critical sizes for coercivity and remanence, *J. Geophys. Res.*, *104*, 617–628.

Pauthenet, R., and L. Bochirol (1951), Aimantation spontanée des ferrites, *J. Phys. Radiat.*, *12*, 249–251.

Petersen, N., D. Weiss, and H. Vali (1989), Magnetotactic bacteria in lake sediments, in *Geomagnetism and Paleomagnetism*, edited by F. Lowes, pp. 231–241, Springer, New York.

Rave, W., K. Fabian, and A. Hubert (1998), Magnetic states of small cubic particles with uniaxial anisotropy, *J. Magn. Magn. Mater.*, *190*, 332–348.

Shcherbakov, V. P., and V. V. Shcherbakova (1975), On magnetostatic interaction in a system of single-domain grains, *Izv. Akad Nauk SSSR Fiz. Zemli*, *9*, 101–104.

Spring, S., U. Lins, R. Amann, K. H. Schleifer, L. C. S. Ferreira, D. M. S. Esquivel, and M. Farina (1998), Phylogenetic affiliation and ultrastructure of uncultured magnetic bacteria with unusually large magnetosomes, *Arch. Microbiol.*, *169*, 136–147.

Suess, D., V. Tsiantos, T. Schrefl, J. Fidler, W. Scholz, H. Forster, R. Dittrich, and J. Miles (2002), Time resolved micromagnetics using a preconditioned time integration method, *J. Magn. Magn. Mater.*, *248*, 298–311.

Taylor, A. P., and J. C. Barry (2004), Magnetosomal matrix: Ultrafine structure may template biomineralization of magnetosomes, *J. Microsc.*, *213*, 180–197.

Taylor, A. P., J. C. Barry, and R. I. Webb (2001), Structural and morphological anomalies in magnetosomes: Possible biogenic origin for magnetite in ALH84001, *J. Microsc.*, *201*, 84–106.

Weiss, B. P., S. S. Kim, J. L. Kirschvink, R. E. Kopp, M. Sankaran, A. Kobayashi, and A. Komeili (2004), Magnetic tests for magnetosome chains in Martian meteorite ALH84001, *Proc. Natl. Acad. Sci. U. S. A.*, *101*, 8281–8284.

Williams, W., and D. J. Dunlop (1989), Three-dimensional micromagnetic modelling of ferromagnetic domain structure, *Nature*, *337*, 634–637.

Williams, W., A. R. Muxworthy, and G. A. Paterson (2006), Configurational anisotropy in single-domain and pseudosingle-domain grains of magnetite, *J. Geophys. Res.*, doi:10.1029/2006JB004556, in press.

Witt, A., K. Fabian, and U. Bleil (2005), Three-dimensional micromagnetic calculations for naturally shaped magnetite: Octahedra and magnetosomes, *Earth Planet. Sci. Lett.*, *233*, 311–324.

Wright, T. M., W. Williams, and D. J. Dunlop (1997), An improved algorithm for micromagnetics, *J. Geophys. Res.*, *102*, 12,085–12,094.

A. R. Muxworthy, Department of Earth Science and Engineering, Imperial College, South Kensington Campus, London, SW7 2AZ, UK. (adrian.muxworthy@imperial.ac.uk)

W. Williams, Grant Institute of Earth Science, University of Edinburgh, Kings Buildings, West Mains Road, Edinburgh, EH9 3JW, UK.